Article

Research on Durability and Prestress Loss of Lightweight Aggregate Concrete Prestressed Box Girders

How-Ji Chen , Cheng-Chang Kuo , Chao-Wei Tang *

Posted Date: 4 September 2023

doi: 10.20944/preprints202309.0067.v1

Keywords: lightweight aggregate concrete; durability; prestress loss; prestressed box girder; creep; shrinkage; chloride ion

Article

Research on Durability and Prestress Loss of Lightweight Aggregate Concrete Prestressed Box Girders

How-Ji Chen [1], Cheng-Chang Kuo [1] and Chao-Wei Tang [2,3,4,*]

[1] Department of Civil Engineering, National Chung-Hsing University, 145 Xingda Road, South District, Taichung City 40227, Taiwan; hojichen@dragon.nchu.edu.tw (H.-J.C.); cchkuo@freewaygov.tw (C.-C.K.)
[2] Department of Civil Engineering and Geomatics, Cheng Shiu University, No. 840, Chengching Road, Niaosong District, Kaohsiung 83347, Taiwan; 0666@gcloud.csu.edu.tw
[3] Center for Environmental Toxin and Emerging-Contaminant Research, Cheng Shiu University, No. 840, Chengching Road, Niaosong District, Kaohsiung 83347, Taiwan
[4] Super Micro Mass Research and Technology Center, Cheng Shiu University, No. 840, Chengching Road, Niaosong District, Kaohsiung 83347, Taiwan
* Correspondence: tangcw@gcloud.csu.edu.tw; Tel.: +886-7-735-8800

Abstract: This study aimed to compare the differences in durability and prestress loss between normal-weight concrete (NC) and lightweight aggregate concrete (LWC) prestressed box girders, which were constructed at the same time in the same area, so as to verify the superiority of using synthetic lightweight aggregate (LWA) made from reservoir sediments in prestressed bridges. For the NCs and LWCs used in prestressed box girders, the basic mechanical properties were tested on the one hand, and the durability properties were tested on the other hand. Then, through the prestress monitoring system, the prestress loss of the two groups of the prestressed box girders was tracked. The results of the durability test confirmed that LWC can inhibit the penetration of air, water, and chloride ions by strengthening the interfacial transition zone between the aggregate and the cement paste, thereby improving its durability. Moreover, the magnetic flux prestress loss of the NC prestressed box girder reached 8.1%. In contrast, the magnetic flux prestress losses on both sides of the LWC prestressed box girder were 4.6% and 4.9%, respectively. This verified that, under the same environmental conditions, the use of LWC produced less of a prestress loss than the use of NC.

Keywords: lightweight aggregate concrete; durability; prestress loss; prestressed box girder; creep; shrinkage; chloride ion

1. Introduction

Lightweight aggregate (LWA) is a general term for natural or synthetic aggregates with a weight from 80 to 900 kg/m^3 [1]. Lightweight aggregate concrete (LWC) can be produced by using LWAs instead of normal-weight aggregates [2]. In the early stage of the development of LWCs, the LWAs used were mainly natural LWAs, the strength level of the concrete was low, and it was mainly used to make thermal insulation bricks. Since S. J. Hayde invented the technology of producing expanded clay LWAs in a rotary kiln in 1917, the progress of synthetic LWA technology has promoted the improvement of the quality of LWAs, thereby accelerating the development of high-strength LWC technology [3]. In the past two decades, in order to reduce the consumption of natural resources, the source of materials for the production of synthetic LWAs has developed toward resource recycling [4]. At present, the development of synthetic LWAs mainly uses industrial waste or municipal solid waste as raw materials. For example, slag, fly ash, reservoir sediment, waste TFT-LCD glass powder, paper sludge, tile grinding sludge, water purification sludge, textile sludge, and other renewable resources are used to produce LWAs [5–18].

According to the performance of LWAs, it can be divided into ordinary LWAs, ultra-light LWAs, high-strength LWAs, and high-performance LWAs. Among them, the shell layer of synthetic high-strength LWAs and high-performance LWAs is hard and dense, but the interior is porous; thus, it is

light in weight and has appropriate strength. Generally speaking, a particle density of sintered synthetic LWAs that is less than 880 kg/m^3 is mostly used to make heat insulation elements; meanwhile, those between 880-1120 kg/m^3 can be used as structural concrete. Therefore, LWCs that are mixed with these excellent synthetic LWAs have the advantages of being lightweight, as well as having heat insulation, fire resistance, seismic resistance, and high-strength properties [19]. The unit weight of LWCs is greatly affected by the type of LWAs, the composition of materials, and the environmental conditions of conservation. The greater the density of LWA used to formulate the concrete, the higher the unit weight of the concrete. In addition, the higher the amount of ordinary sand used in LWCs, the greater its unit weight. For the maximum limit of LWC unit weight, the relevant standards of various countries have clear regulations according to their respective resource conditions and technical requirements. For example, according to ACI 213R-14 [20], structural LWC is defined as a 28-day compressive strength exceeding 17 MPa and a 28-day air-dried unit weight not exceeding 1850 kg/m^3.

In concrete, the quality of the aggregate–paste interface is a key factor affecting its long-term durability. Expanded shale, clay, and slate LWAs are highly absorbent, yet they are composed of vitrified silicates and are particularly durable [21]. In addition, LWAs have other unique properties that can improve the durability of LWCs, such as the elastic compatibility between LWAs and cement paste, the ability of LWAs to promote internal curing, and the lower rigidity of LWAs [21]. In particular, a relatively dense interfacial transition zone (ITZ) is formed between LWAs and cement paste, which results in LWCs having good durability. Many studies have shown that the ITZ of LWCs is much better than that of NCs, which is due to the improved adhesion between LWAs and cement paste [22–30]. On the other hand, structural LWCs can provide a more effective strength ratio (ratio of strength to weight) than normal-weight concretes (NC). Therefore, structural LWCs with a unit weight of 1400-2200 kg/m^3 have been widely used in various structural projects such as high-rise buildings, bridges, prestressed members, and offshore oil platforms, and the use of it in these contexts has shown good development and prospects [20,31]. However, the basic components of LWCs, their interactions, and their effects on mechanical properties and durability are significantly different from those of NCs [32]. This difference is attributed to the composition of the mortar matrix and the LWAs used [33,34]. In NCs, the elastic modulus and strength of normal-weight aggregates are greater than that of mortar, and the aggregate is the main load-bearing system. Once the applied stress exceeds the tensile strength of the mortar, the mortar will crack first and penetrate the whole mortar [35,36]. In contrast, when LWC is stressed, the situation is more complicated, as it depends on the elastic modulus of LWAs and whether its strength is higher or lower than that of mortar [37]. Therefore, the complex relationship between the two materials makes the mechanical behavior and collapse mechanism of LWCs applied to reinforced concrete and prestressed concrete members quite different from that of NC [38]. For example, typical expanded clay LWA has an elastic modulus in the range of 10 to 20 GPa, while ordinary aggregates range from about 30 to 100 GPa—this is the most important difference between the LWCs and NCs used in prestressed members [39]. In general, the elastic modulus of LWCs may be 15–60% lower than that of NCs of the same strength class, depending on the density of the concrete and the aggregate used [40,41]. In view of this, certain design codes have put forward specific suggestions for structural LWC, as well as have evaluated reinforced LWC members by means of their strength reduction coefficients [42]. Most of the reduction values are based on the experimental results of traditional LWC members. For example, the ACI 318 building code [43] uses a correction factor based on the density of the concrete to account for the elastic modulus, tensile strength, shear strength, and torsional strength of LWCs in comparison to NCs with the same compressive strength.

Many studies have shown that LWCs perform much better than NCs under variable and dynamic loads [44,45]. In particular, the lighter structure of LWCs ensures higher natural frequencies, lower vibration amplitudes, and higher damping. Therefore, the application of LWCs in bridge engineering has been quite common [46]. Furthermore, LWCs have a small self-weight, which can reduce the bending moment of the prestressed beam and the bridge deck, thereby reducing the section of the component that is used to achieve a larger span. In prestressed members, prestressing

is the application of compressive stress to concrete in order to relieve the tensile strain caused by a load. For prestressed concrete structures, information on the actual state of prestress is an important basis for determining their load-carrying capacity and remaining service life [47]. Prestress loss refers to the slow reduction in the induced compressive stress in a prestressed part due to various factors. The various reductions in the prestressing force are called the losses in prestressing, and it is an important topic in the design of prestressed members. There are two main types of prestress loss, immediate (short term) and time-dependent (long term), and these apply depending on the time and duration of their occurrence. The first type is the instantaneous elastic shortening loss; the second type is the long-term loss, which is mainly caused by the relaxation of the prestressing strands that results in a creep and shrinkage of the concrete [48,49]. Prestress loss is also affected by other time-dependent concrete properties, such as compressive strength and the modulus of elasticity. Bymaster et al. [50] advised that LWCs have a large prestress loss. This is due to the lower elastic modulus of LWAs with lower stiffness, thereby leading to the expected greater elastic shortening of LWC members. Chen et al. [19] tested the performance of self-consolidating lightweight aggregate concrete (SCLC) and prestressed SCLC members, and compared them with members of normal-weight self-consolidating concrete (SCC). Their test results showed that, after 180 days of prestressing, the prestress loss of full-scale SCLC members was around 5.35%-6.83%, which was lower than that of conventional SCC members (approximately 8.19%-9.06%). Kraľovanec et al. [47] concluded that the prestress loss of the prestressed components is affected by the construction stage, the materials used, the prestressing technology, or the required service life of the component.

For accurate prestress loss prediction, it is especially important to understand the creep and shrinkage behavior of concrete [51]. In other words, the creep and shrinkage control of concrete are other important factors that affect the performance of prestressed concrete members [35,36,52,53]. In terms of time-dependent properties such as shrinkage and creep, most researchers recognize that shrinkage and creep are always higher for LWCs than for NCs [52,54–56]. This is because the stiffness (that is, elastic modulus) of LWAs itself is lower than that of ordinary aggregates, which makes the restraining effect of aggregates on the autogenous shrinkage of cementitious materials weaker, thus resulting in larger drying shrinkage and degree of creep in LWCs than in NCs. Report BE 96-3942/R2 [57] stated that the creep strain of LWCs is maybe 20-60% higher compared to concrete with normal-weight aggregates. However, the results of Nilsen and Aitcin [58] showed that the drying shrinkage of LWCs made of expanded shale was 30% to 50% lower than that of NCs. Furthermore, Lopez et al. [59] showed that high-performance LWCs mixed with expanded slate LWAs exhibited less creep and slightly greater shrinkage than the general HPC of similar paste, mix design, and strength. Rodacka et al. [60] showed that the final value of the test for the shrinkage deformation of LWCs was 38% lower than the value estimated according to Eurocode EN-1992-1-1 [61]. Furthermore, the final creep deformation of the tested LWCs was more than two times lower than that of the corresponding NCs. Szydłowski and Łabuzek [38] presented the results of the study on the creep and shrinkage of LWCs. A creep test of 539 days under a prestressed load showed a particularly low creep coefficient; a shrinkage test was then carried out for 900 days, which also exhibited low shrinkage. Compared with NCs, LWCs with higher strength, especially high-strength LWCs, can exhibit similar—and sometimes even lower—creep strains [62–64]. This is because the matrix of LWC usually has higher strength than the matrix of the same grade of NC, which makes the creep of the matrix less. Kayali [64] showed that different types of LWAs produce distinct drying shrinkage behaviors. In general, whether it is LWC or NC, the higher the compressive strength, the lower the creep [60].

In the past two decades, Taiwan has successfully sintered LWAs with excellent properties from reservoir sediment and applied them to structural engineering [8–10]. In order to verify the feasibility of applying synthetic LWAs from reservoir sediments to prestressed bridges, the Taiwan Highway Bureau selected an interchange bridge located in central Taiwan (as shown in Figure 1), and this was achieved using concrete poured with synthetic LWAs as the structural material. In view of the importance of evaluating the prestress loss and durability in prestressed concrete structures, a monitoring plan for an LWC-prestressed box bridge with a span of 40 meters in the viaduct was implemented. On the other hand, another NC prestressed box bridge with a similar structural cross

Preprints (www.preprints.org) | NOT PEER-REVIEWED | Posted: 4 September 2023 doi:10.20944/preprints202309.0067.v1

section was selected from another adjacent bridge section (as shown in Figure 1), and the same monitoring and testing operations were carried out as a control group. The standard cross section and longitudinal section of the NC and LWC prestressed box girders are shown in Figure 2 and Figure 3, respectively.

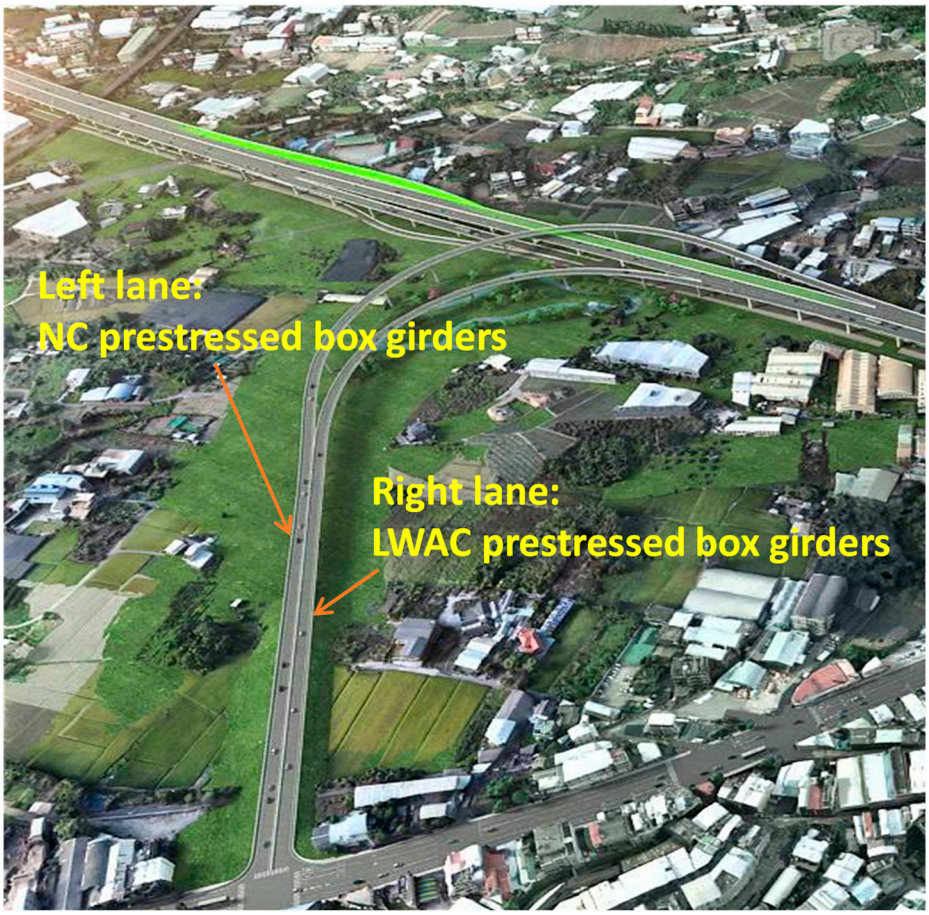

Figure 1. Schematic diagram of the location of the NC and LWC prestressed box girders.

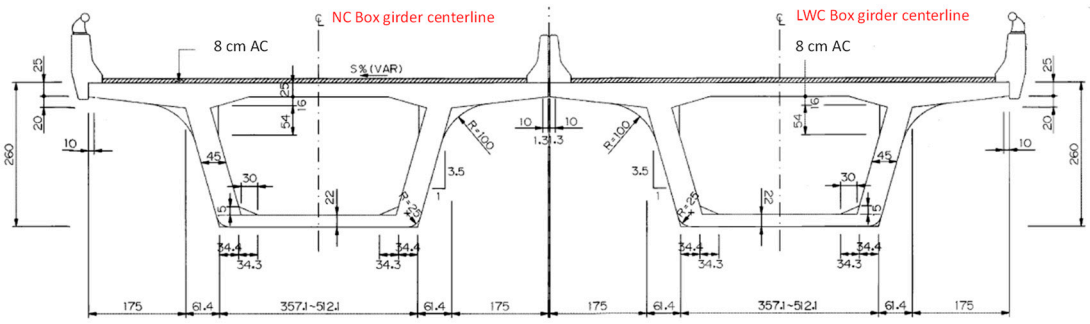

Figure 2. Standard cross section of the NC and LWC prestressed box girders.

Preprints (www.preprints.org) | NOT PEER-REVIEWED | Posted: 4 September 2023 doi:10.20944/preprints202309.0067.v1

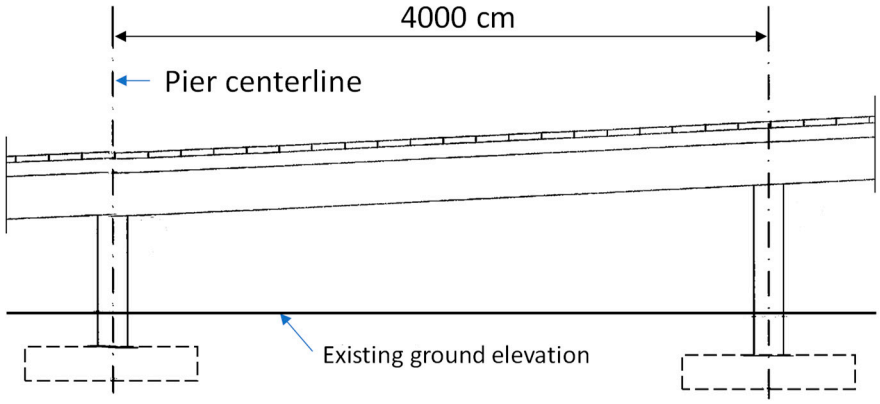

Figure 3. Standard longitudinal section of the NC and LWC prestressed box girders.

In this study, according to the construction progress of the bridge, magnetic flux monitoring instruments were installed on site to monitor the pre-stress changes in the pre-stressed steel tendons in the bridge components over a long period of time. In addition, the time-dependent deformation and durability test results of the concrete at the construction site and in the laboratory were analyzed. The monitoring and testing of the related items of this study included various property tests of the concrete (basic performance, time-dependent deformation, and durability) and monitoring of the pre-stress loss of pre-stressed steel tendons. The results obtained from this actual monitoring and testing can be used as a reference for Taiwan to promote the design of lightweight aggregate prestressed concrete bridges in the future.

2. Materials and Methods

2.1. Materials

The materials used in this study and their sources are described below:

- Cement: a locally produced Type I Portland cement, with a specific gravity of 3.15 and a fineness of 3550 cm^2/g;
- Slag: purchased from Yu Qingtang Enterprise, and its specific gravity was 2.89;
- Fly ash: taken from Taichung Thermal Power Plant, and its specific gravity was 2.32;
- Silica fume: purchased from Elkem Taiwan, and its specific gravity was 2.1;
- Water: general tap water, which is in line with the general quality requirements of concrete mixing water;
- Fine aggregate: a natural river sand with an FM value of 2.67, a specific gravity of 2.63, and a 24-hour water absorption rate of 1.3%;
- Coarse aggregate: a natural crushed stone with a specific gravity of 2.64 and a 24-hour water absorption rate of 0.7%;
- Lightweight aggregate: the appearance of the synthetic LWA obtained by using reservoir sediments used in this study is shown in Figure 4, and its basic properties are shown in Table 1;
- Superplasticizer: purchased from An-Yao Company, and it met the requirements of ASTM C494-81 Type F.

Figure 4. Appearance of synthetic LWAs that were created using reservoir sediments.

Preprints (www.preprints.org) | NOT PEER-REVIEWED | Posted: 4 September 2023 doi:10.20944/preprints202309.0067.v1

Table 1. Basic properties of lightweight aggregates.

Items		Test Value	Test Method
Bulk specific gravity		1.32	ASTM C127 [65]
Crushing strength		4.9 MPa	CNS 14779 [66]
Los Angeles abrasion value of aggregate		31.20%	CNS 490 [67]
Soundness of aggregate via use of sodium sulfate or magnesium sulfate		0.11%	CNS 1167 [68]
Water absorption rate	24-hour	10%	ASTM C127 [65]
	48-hour	12%	
Dry unit weight		835 kg/m^3	CNS 3691 [69]

2.2. Mix Proportions of Concrete

In this study, the specimens of the control group (NC) and the experimental group (LWC) were made, respectively. Considering the workability, strength, and durability of concrete, the amount of each material of the two groups of concrete was determined by trial mixing. The mix proportions of the two groups of concrete are shown in Table 2.

Table 2. Mix proportions of the concretes (kg/m^3).

Concrete Group	W/B	W	C	SL	FA	SF	LWA	CA	FA	SP
Control group	0.36	163	364	90	0	0	0	971	774	5.0
Experimental group	0.39	210	296	162	54	27	465	0	615	4.85

Notes—W/B: water–binder ratio; W: water; C: cement; SL: slag; FA: fly ash; SF: silica fume; LWA: lightweight aggregate; CA: coarse aggregate; FA: fine aggregate; and SP: superplasticizer.

2.3. Casting and Curing of Specimens and Test Methods

During the pouring operation of the bridge, the sampling of two groups of concrete and the preparation of specimens were carried out simultaneously for subsequent concrete property tests. The test items and specimen ages, as well as the test specifications of the basic properties and time-dependent deformation of concrete are shown in Table 3. After pouring the specimens on-site, the specimens were divided into two parts. One was for on-site curing, which kept the specimen moist with mist spray for 7 days. After that, the specimens were subjected to air curing. The other part was for laboratory standard curing. The temperature in the curing room was controlled at 23 ± 2 °C, and the relative humidity was greater than 95%. The specimens were taken out one day before the planned curing age for various basic property tests.

Table 3. The test items, specimen ages, and test specifications of the basic properties and time-dependent deformation of the concretes.

Test Items	Specimen Ages (Day)	Specimen Size	Test Specifications
Air-dry unit weight	90	Cylinders (15 cm × 30 cm)	ASTM C567
Compressive strength	28, 56, 90, 180	Cylinders (15 cm × 30 cm)	ASTM C39
Flexural strength	28, 56, 90, 180	Prisms (15 cm × 15 cm × 53 cm)	ASTM C78
Splitting tensile strength	28	Cylinders (15 cm × 30 cm)	ASTM C496

Preprints (www.preprints.org) | NOT PEER-REVIEWED | Posted: 4 September 2023 doi:10.20944/preprints202309.0067.v1

Elastic modulus	28, 56, 90, 180	Cylinders (15 cm × 30 cm)	ASTM C469
Drying shrinkage	0, 14, 28, 56, 90, 180, 360	Prisms (7.5 cm × 7.5 cm × 28 cm)	ASTM C157
Creep	0, 14, 28, 56, 90, 180, 360	Cylinders (15 cm × 30 cm)	ASTM C512

The air-dry unit weight of concrete cylinders (15 cm × 30 cm) at the age of 90 days was measured according to the ASTM C567 [70]. The concrete specimens were tested for compressive strength (ASTM C39 [71]), flexural strength (ASTM C78 [72]), splitting tensile strength (ASTM C496 [73]), elastic modulus (ASTM C469 [74]), drying shrinkage (ASTM C157 [75]), and creep strain (ASTM C512 [76]). The specimens of the drying shrinkage test adopted the on-site curing method, and the test equipment and specimens are shown in Figure 5. In addition, the specimens of the creep test also adopted the on-site curing method.

(a) (b)

Figure 5. Drying shrinkage test: (a) equipment and (b) specimens.

In terms of concrete durability tests, the test items, specimen ages, and test specifications of concrete durability are shown in Table 4. There were three test ages for each group of concrete, and three specimens were poured for each age. After 24 hours of casting, the specimens were de-molded. Afterward, the specimens were subjected to laboratory standard curing until they were taken out one day before the planned age. Thereafter, various durability tests were performed.

Table 4. The test items, specimen ages, and test specifications of concrete durability.

Test Items	Specimen Ages (Day)	Specimen Size	Test Specifications
Ultrasonic pulse velocity test	28, 90, 180	Cylinders (10 cm × 20 cm)	ASTM C597
Concrete's ability to resist chloride ion penetration test	28, 90, 180	Cylinders (10 cm × 20 cm)	CNS 14795
Chloride ion penetration test	28, 90, 180	Cylinders (10 cm × 20 cm)	ASTM C1543 and CNS 15649
Scanning electron microscope observation	28, 90, 180	Fragments after concrete compression test	ACI 213R-14

The ultrasonic test was carried out with reference to ASTM C597 [77]. The ultrasonic wave was transmitted through the instrument to penetrate the concrete specimen to detect its wave velocity, thus estimating the compactness of the concrete. The anti-chloride ion penetration test was carried out with reference to CNS 14795 [78]. During the 6-hour test period, the current passing through a concrete sample with a thickness of 5 cm and a nominal diameter of 10 cm was measured (as shown

Preprints (www.preprints.org) | NOT PEER-REVIEWED | Posted: 4 September 2023 doi:10.20944/preprints202309.0067.v1

in Figure 6). After calculating the total passing electricity, the current was expressed in coulombs to evaluate the ability of the concrete to resist the penetration of chloride ions.

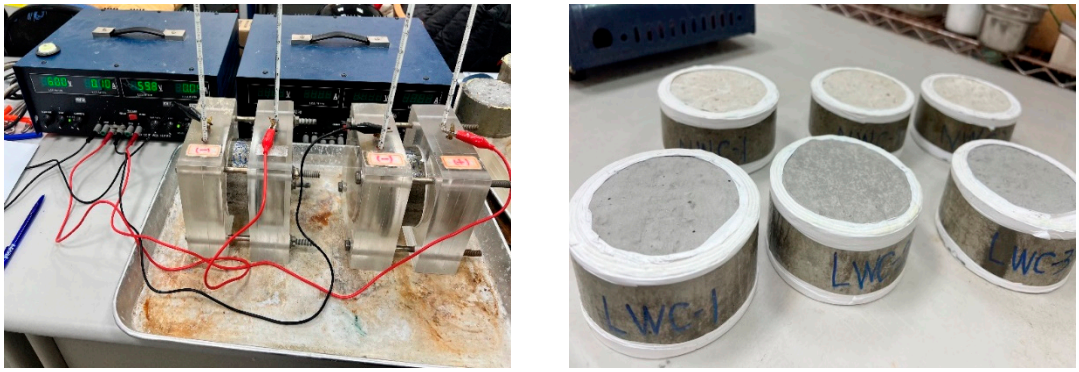

(a) (b)

Figure 6. Rapid chloride permeability test: (a) equipment and (b) specimens.

The chloride ion penetration test was carried out according to ASTM C1543 [79] and CNS 15649 [80]. The size of the specimen was 15 × 15 × 15 cm, and its center was hollowed out, as shown in Figure 7. A 3% sodium chloride solution was poured into the center of the concrete specimen. After the concrete was soaked, the sample slices were taken out according to the required depth and ground. According to CNS 14702 [81], the content of the chloride ions was measured. Among them, the specimens not immersed in the solution were used for comparison. In addition, the crumble at the junction of the aggregate and the cement paste in the center of the cylinder after the compression test was taken as a sample for microscopic observation with an electron microscope.

(a) (b)

Figure 7. Chloride ion penetration test: (a) situation following specimen pouring and (b) the specimens containing sodium chloride solution.

2.4. Prestress Loss Monitoring of Prestressed Tendons

The configuration of the prestressed tendons of the NC and LWC prestressed box girders is shown in Figure 8. In this study, a magnetic flux cable force measurement system was used to monitor the prestress loss of the tendon of prestressed concrete box girders. Using a magnetic flux sensor to measure tendon preload is a new method that has been tried in recent years. The measurement principle is based on the fact that the stress on steel is the main sensitive factor that directly affects its magnetic permeability. Therefore, the pre-force value can be calculated by measuring the change in the magnetic permeability of the tendon. When the magnetoelasticity instrument applies a pulse voltage signal to the exciting coil, the exciting coil will generate a magnetic field in the tendon, and—at the same time—an induced voltage will be generated in the measuring coil. When the tendon is changed by the stress of the load, the magnetic field strength inside the tendon will also change, and—at the same time—the induced voltage in the measuring coil will also change. Therefore, the magnetoelastic instrument detects the slight change in the induced voltage on the measuring coil,

Preprints (www.preprints.org) | NOT PEER-REVIEWED | Posted: 4 September 2023 doi:10.20944/preprints202309.0067.v1

calculates the force of the tendon, and then displays it on the instrument. The installation diagram of the magnetic flux CCT-120 sensor used in this study is shown in Figure 9.

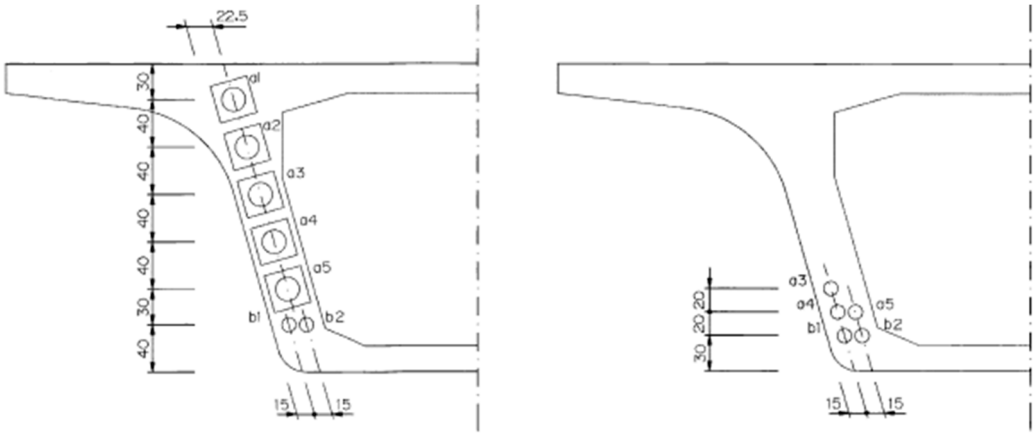

(a) (b)

Figure 8. The configuration of prestressed tendons: (a) support end and (b) span center.

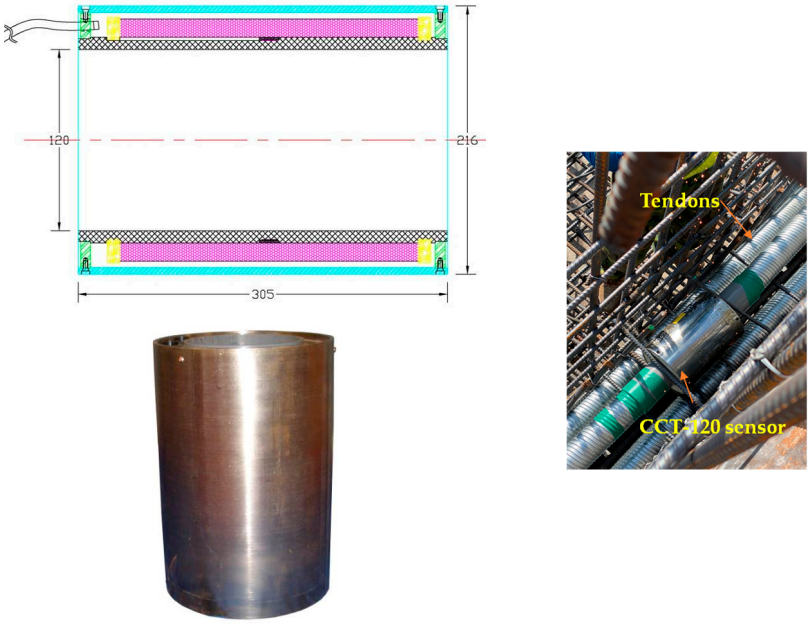

(a) (b)

Figure 9. Magnetic flux cable force measurement system: (a) CCT-120 sensor and (b) configuration.

3. Results and Discussion

3.1. Test Results of the Basic Properties and Time-Dependent Deformation of Concrete

3.1.1. Results of the Air-Dried Unit Weight and Compressive Strength Tests

The test results of the air-dried unit weight of the two groups of concrete are shown in Table 5. Under the standard curing and on-site curing modes, the air-dried unit weights of the NCs were 2391 and 2333 kg/m^3, respectively, while those of LWC were 1817 and 1820 kg/m^3, respectively. This shows that the unit weight of the LWCs was only about 76%-78% of the NCs, which meant that replacing NC with LWC could reduce the weight of the whole structure by more than 20%, thereby achieving the purpose of reducing the inertial force during earthquakes. In addition, according to ACI 213R-14 [20], the test results of this study showed that the air-dried unit weight did not exceed 1850 kg/m^3.

Preprints (www.preprints.org) | NOT PEER-REVIEWED | Posted: 4 September 2023 doi:10.20944/preprints202309.0067.v1

Table 5. Test results of the air-dried unit weight and compressive strength of the concretes.

Groups	Curing Method	Compressive Strength (MPa)				Air-Dried Unit Weight (kg/m³)
		28 Days	56 Days	90 Days	180 Days	90 Days
NC	Standard curing	58.8	68.9	74.5	75.1	2391
	On-site curing	61.6	65.4	64.7	67.1	2333
LWC	Standard curing	47.1	50.6	52.4	56.1	1817
	On-site curing	51.0	51.6	52.4	53.3	1820

The compressive strength test results are shown in Table 5. It can be seen from Table 5 that the 28-day compressive strength of the LWCs in this study exceeded 17 MPa, which meet the requirements of ACI 213R-14 [20]. Moreover, it can be seen from Figure 10 that the strength of the two groups of concrete increased with age, especially under standard curing. Under standard curing, the improvement of concrete strength was particularly obvious. This is consistent with the research results of Wang et al. [82]. This is due to the standard curing process, which prevents or replenishes the loss of moisture in the concrete while maintaining a temperature that is conducive to hydration. Under the two different curing modes, the increase in the compressive strength of the LWC was smaller than that of the NC. Under standard curing, the 28-day compressive strength of the LWC was 47.1 MPa, and the 90-day compressive strength was 52.4 MPa. In two months, the strength increased by only 11.3%, which was significantly less than the 26.7% increase in the NC. This is consistent with the research results of Al-Khaiat and Haque [83], that is, LWC grows faster than NC in terms of early strength. In addition, there was a relative increase in the early strength of the field-cured specimens. However, the long-term exposure to outdoor sunlight and poor curing conditions caused the strength growth of the specimens to slow down in the later stage. In contrast, the specimens treated with standard curing had a more than enough hydration reaction, thus making the strength of longer ages higher than that of the on-site curing.

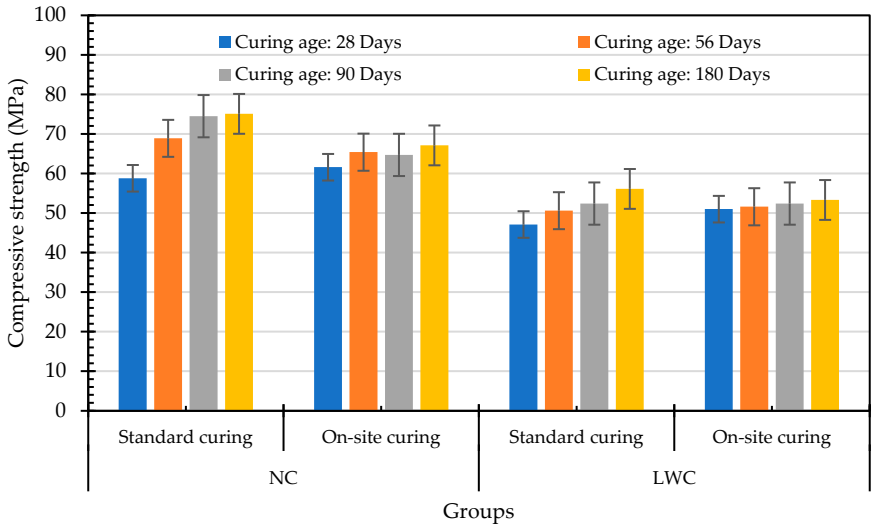

Figure 10. Relationship between the compressive strength and curing age.

3.1.2. Results of the Flexural Strength and Splitting Tensile Strength Tests

The test results of the flexural strength are shown in Table 6. All fracture surfaces were located within 1/3 of the span of the center of the specimen, indicating that the mixing and pouring of the specimen was quite uniform. The flexural strength of the LWC calculated according to the ACI 318 suggested formula was 3.6 MPa, while the flexural strength of LWC obtained in this study was between 3.5-4.6 MPa. It can be seen from Figure 10 that the flexural strength of the two groups of concrete increased with age. Under standard maintenance, the 28-day flexural strength of LWC was 3.5 MPa, and the 90-day flexural strength was 4.3 MPa. In two months, the strength increased by

Preprints (www.preprints.org) | NOT PEER-REVIEWED | Posted: 4 September 2023 doi:10.20944/preprints202309.0067.v1

22.9%, slightly higher than the 20.9% of the NC. In addition, regardless of the age, the flexural strength of the standard curing of the two groups of concrete was greater than that of the on-site curing. At the age of 28 days, the flexural strength of the LWC with standard curing was 3.5 MPa, and that of the on-site curing was 3.0 MPa. Compared with the compressive strength, it was about 6%-7% of the compressive strength. At the age of 28 days, the flexural strength of the NC with standard curing was 6.7 MPa, and that of on-site curing was 6.2 Mpa. Compared with the compressive strength, it was about 10%-11% of the compressive strength. The results showed that NC was superior to LWC in flexural strength.

Table 6. Test results of the flexural strength and splitting tensile strength of the concretes.

Groups	Curing Method	Flexural Strength (MPa)				Splitting Tensile Strength (MPa)
		28 Days	56 Days	90 Days	180 Days	28 Days
NC	Standard curing	6.7	7.0	8.1	8.8	4.6
	On-site curing	6.2	7.1	7.1	7.9	4.5
LWC	Standard curing	3.5	3.9	4.3	4.6	3.0
	On-site curing	3.0	2.8	3.0	4.0	2.3

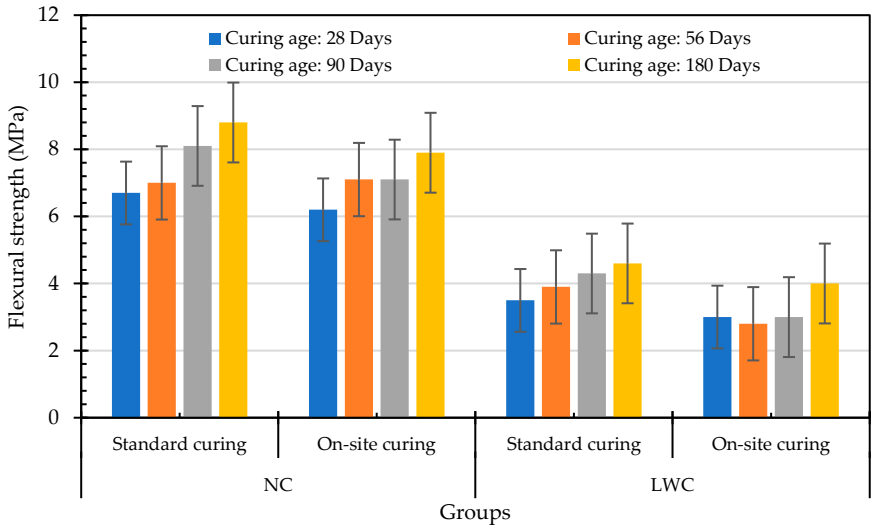

Figure 11. Relationship between the flexural strength and curing age.

The test results of the splitting tensile strength are shown in Table 6. At the age of 28 days, the splitting tensile strength of the LWC with standard curing was 3.0 MPa, and that of on-site curing was 2.3 MPa, it was about 4%-7% of the compressive strength. At the age of 28 days, the flexural tensile strength of NC with standard curing was 4.6 MPa, and that of site curing was 4.5 MPa. Compared with the LWC, it was about 7%-8% with respect to the compressive strength. It can be seen that the splitting tensile strength of NC was relatively excellent, which was in line with the recommendation of ACI 213R-14 [20].

3.1.3. Results of Elastic Modulus Test

The test results of elastic modulus are shown in Table 7. Under two different curing modes, the elastic modulus of LWC at different curing ages ranged from 21.4 to 29.2 GPa. These values are consistent with the experimental results reported in the literature [39,84]. In addition, the modulus of

Preprints (www.preprints.org) | NOT PEER-REVIEWED | Posted: 4 September 2023 doi:10.20944/preprints202309.0067.v1

elasticity of the two groups of concrete increased with age, as shown in Figure 12. The improvement under standard curing was particularly evident, and the improvement rate of LWC was relatively high. Overall, the elastic modulus of the LWC was about 60%-70% of that of NC. This is consistent with the literature [40,41].

Table 7. Test results of the elastic modulus of the concretes.

Groups	Curing Method	Elastic Modulus (GPa)			
		28 Days	56 Days	90 Days	180 Days
NC	Standard curing	36.1	37.4	37.5	40.5
	On-site curing	36.5	35.0	38.2	39.6
LWC	Standard curing	23.0	24.6	25.8	29.2
	On-site curing	21.7	21.4	22.1	25.2

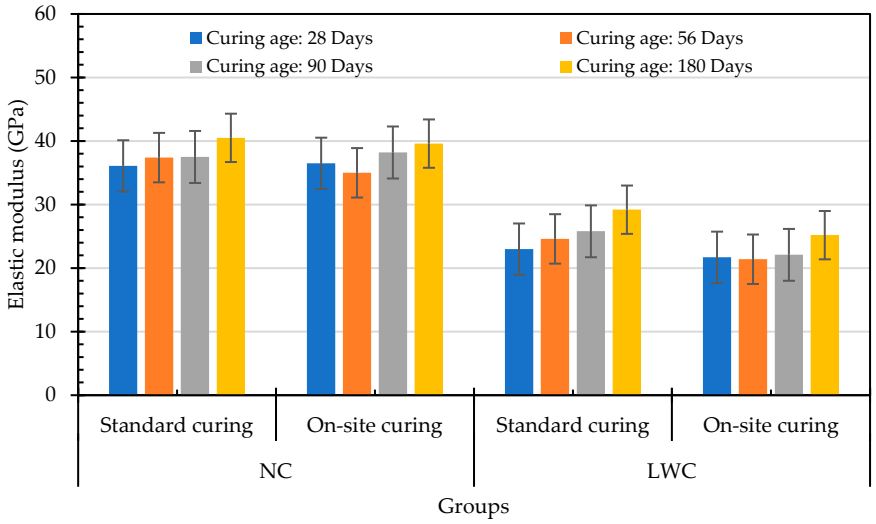

Figure 12. Relationship between the elastic modulus and curing age.

3.1.4. Results of the Drying Shrinkage Test

The results of the drying shrinkage test are shown in Table 8. The initial drying shrinkage of NC was relatively severe, but it slowed down after 90 days, as shown in Figure 13. This is due to the low permeability of normal-weight aggregates in nature, and that they are less prone to drying shrinkage than cement paste [1]. In contrast, the LWC had a smaller drying shrinkage in the early stage, and the 360-day test age did not slow down, as shown in Figure 12. This is because the LWAs in the LWC slowly released water into the matrix, which made it more able to inhibit the early drying shrinkage, thus making the initial drying shrinkage smaller [21]. Therefore, the drying shrinkage of the LWC at the age of 180 days was 447 μ, which was smaller than that of NC, which is 480 μ. However, at the age of 360 days, the dry shrinkage of the LWC was slightly higher than that of the NC. This finding was consistent with the findings of Lopez et al. [59].

Table 8. Test results of the drying shrinkage of the concretes.

Groups	Drying Shrinkage (μ)						
	0 Days	14 Days	28 Days	56 Days	90 Days	180 Days	360 Days
NC	0	180	261	331	416	480	528
LWC	0	73	137	215	291	447	577

Preprints (www.preprints.org) | NOT PEER-REVIEWED | Posted: 4 September 2023 doi:10.20944/preprints202309.0067.v1

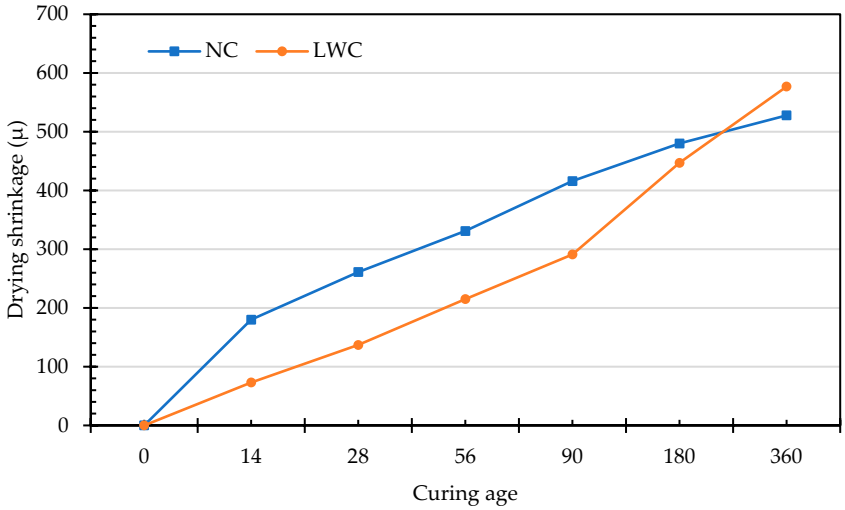

Figure 13. Relationship between the drying shrinkage and curing age.

3.1.5. Results of Creep Test

The results of the creep test are shown in Table 9. The creep of the two groups of concrete was roughly the same, but the early creep of the LWC was more evident than that of NC, as shown in Figure 14. This is because the normal-weight aggregates generally did not exhibit appreciable creep when subjected to stress. These values were consistent with the experimental results reported in the literature [50,54–57]. At the age of 28 days, the creep of the LWC reached 455 μ, which was 69% of that at the age of 360 days and tended to be flat after 90 days. This phenomenon is presumed to be due to the lower elastic modulus of the LWC than that of the NC. Therefore, the creep under initial pressure was larger. Afterward, due to the smaller dry shrinkage, the total creep was equivalent to the NC. This was consistent with the findings of Holste et al. [85].

Table 9. Test results of the creep of the concretes.

Groups	Creep (μ)						
	0 Days	14 Days	28 Days	56 Days	90 Days	180 Days	360 Days
NC	0	317	392	509	582	603	753
LWC	0	400	455	523	597	617	661

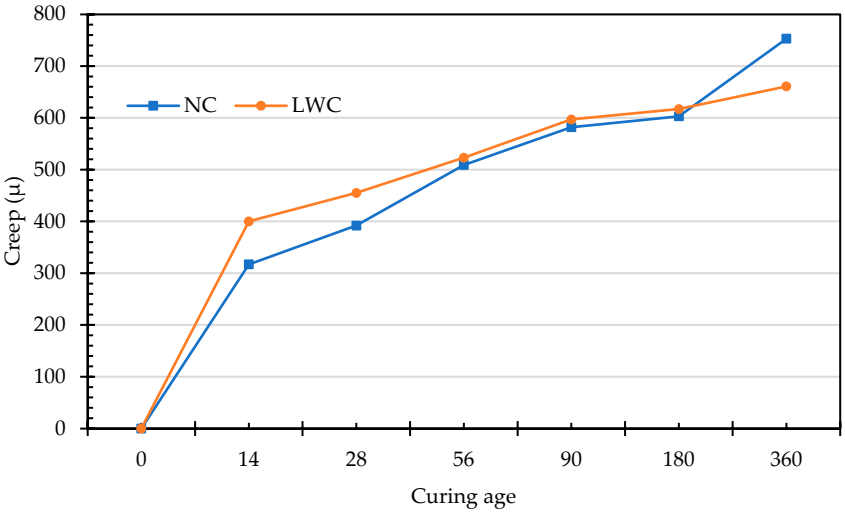

Figure 14. Relationship between the creep and curing age.

Preprints (www.preprints.org) | NOT PEER-REVIEWED | Posted: 4 September 2023 doi:10.20944/preprints202309.0067.v1

In order to understand the creep response of the LWC per unit of compressive stress, the value of its specific creep was also calculated, as shown in Table 10. The specific creep growth trends of the two groups of concrete were particularly similar, as shown in Figure 15. However, the specific creep of the LWC was larger than that of the NC, which means that the response of the LWC to the strain deformation of the pressurized load was more evident.

Table 10. Test results of the specific creep of the concretes.

Groups	Specific Creep (μ/MPa)						
	0 Days	14 Days	28 Days	56 Days	90 Days	180 Days	360 Days
NC	0	22.8	28.3	36.7	42.0	43.5	54.3
LWC	0	36.1	41.0	47.1	53.8	55.6	59.5

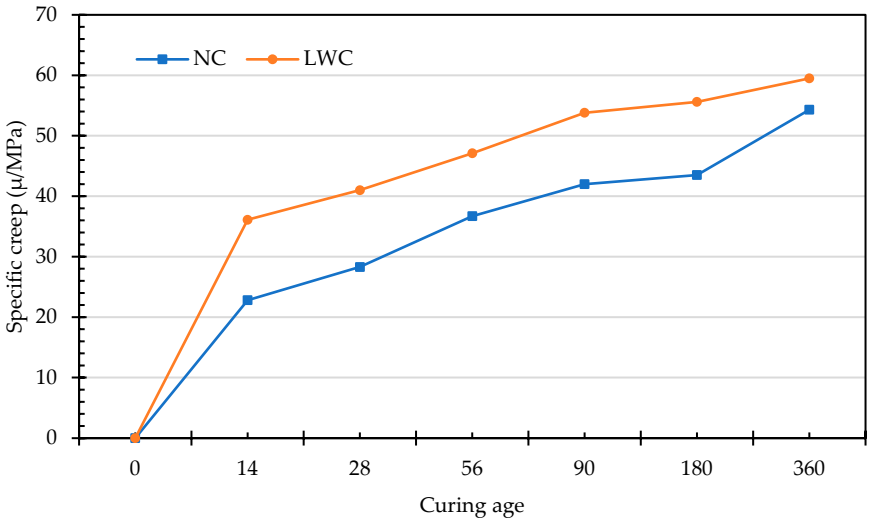

Figure 15. Relationship between the specific creep and curing age.

3.2. Test Results of Concrete Durability

3.2.1. Results of the Ultrasonic Pulse Velocity Test

The results of the ultrasonic pulse velocity test are shown in Table 11. At the age of 28 days and 180 days, the ultrasonic pulse velocity of the LWC was 4048 and 4309 m/s, respectively, while that of the NC was 4469 and 4720 m/s, respectively. The results showed that the ultrasonic pulse velocity of the LWC was lower than that of the NC of the same age. However, according to the recommendation of ASTM C597 (as shown in Table 12), the compactness of the LWC was rated as of a "good" quality.

Table 11. Test results of the ultrasonic pulse velocity of the concretes.

Groups	Curing Age (Day)	Ultrasonic Pulse Velocity (m/s)	Average Ultrasonic Velocity (m/s)
NC	28	4470.4, 4452.8, 4483.2	4469
	90	4608.8, 4604.3, 4682.4	4632
	180	4724.1, 4733.6, 4701.8	4720
LWC	28	4067.5, 4053.7, 4022.4	4048
	90	4252.7, 4188.6, 4231.6	4224
	180	4332.2, 4308.2, 285.7	4309

Preprints (www.preprints.org) | NOT PEER-REVIEWED | Posted: 4 September 2023 doi:10.20944/preprints202309.0067.v1

Table 12. Ultrasonic pulse velocities of the concrete and quality judgments.

UPV Range (m/s)	Concrete Quality
More than 4500	Excellent
From 3600 to 4500	Good
From 3000 to 3600	Questionable
From 2100 to 3000	Poor
From 1800 to 2100	Very poor

3.2.2. Results for the Electrical Indication of the Concrete's Ability to Resist the Chloride Ion Penetration Test

The results of the chloride ion penetration resistance test are shown in Table 13. At the age of 28 and 180 days, the total charges of the LWC were 2889 and 432 coulombs, respectively, while those of the NC were 1002 and 387 coulombs, respectively. According to the recommended judgment value of the chloride ion permeability (Table 14), the NC was classified as having "Very Low" or "Low" chloride permeability. At the age of 28 days, the total charge of the LWC was 2889 coulombs, and the probability of the chloride ion penetration was rated as "Moderate". However, at the age of 180 days, the total charge of the LWC was only 432 coulombs; thus, it was classified as having "Very Low" chloride permeability.

Table 13. Test results of the rapid chloride permeability of the concretes.

Groups	Curing Age (Day)	Average Charge Passed (Coulombs)
NWC	28	1002
	90	603
	180	387
LWC	28	2889
	90	962
	90	432

Table 14. Rapid chloride permeability test ratings.

Charge Passed (Coulombs)	Chloride Ion Penetrability
>4000	High
2000-4000	Moderate
1000-2000	Low
100-1000	Very Low
<100	Negligible

3.2.3. Results of the Chloride Ion Penetration Test

Table 15 shows the results of the chloride ion penetration test. After the LWC was soaked in 3% sodium chloride solution for 180 days, the chloride ions increased by 1.206 and 0.495 kg/m^3 at depths of 1.6-13 mm and 13-25 mm, respectively. However, under the same conditions, the chloride ions of the NC reached 1.490 and 1.420 kg/m^3. The results showed that the increase in chloride ions in the LWC over a depth of 25 mm was much less than that in the NC. In other words, high-strength LWC could effectively resist chloride ion erosion, which is consistent with the results in the literature [86].

Preprints (www.preprints.org) | NOT PEER-REVIEWED | Posted: 4 September 2023 doi:10.20944/preprints202309.0067.v1

Table 15. Test results of the chloride ion penetration test.

Groups	Curing Age (Day)	Increase in Chloride Ion Content (kg/m³)			
		Sampling position: 1.6-13 mm	Difference from the comparison sample	Sampling position: 13-25 mm	Difference from the comparison sample
NC	0	0.030	0.000	0.033	0.000
	28	0.524	0.494	0.293	0.260
	90	1.270	1.240	1.210	1.177
	180	1.521	1.490	1.453	1.420
LWC	0	0.096	0.000	0.076	0.000
	28	0.680	0.584	0.097	0.021
	90	0.918	0.822	0.307	0.231
	180	1.302	1.206	0.571	0.495

3.2.4. Results of the Scanning Electron Microscope Observation

The SEM observation results of the two groups of concrete after curing for 28 and 90 days are shown in Figure 16 and Figure 17, respectively. It can be seen from these figures that there were obvious cracks in the ITZ of the NC. In contrast, the ITZ of the LWC had no visible interfacial cracks. This result showed that the LWC could inhibit the infiltration of air, water, and chloride ions due to the strengthening of the ITZ between the LWAs and cement paste, thus improving its durability.

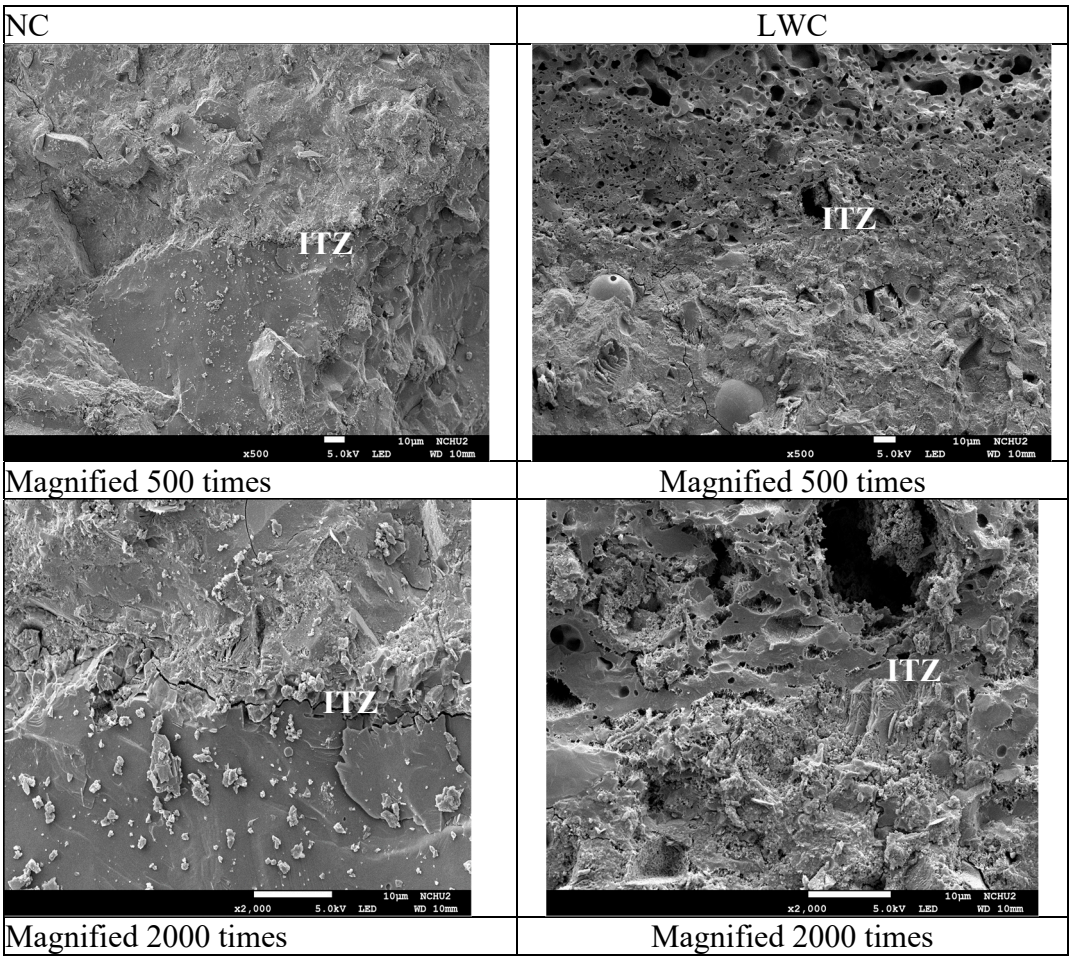

Figure 16. SEM micrographs of the concrete samples with a curing age of 28 days.

NC	LWC

Preprints (www.preprints.org) | NOT PEER-REVIEWED | Posted: 4 September 2023 doi:10.20944/preprints202309.0067.v1

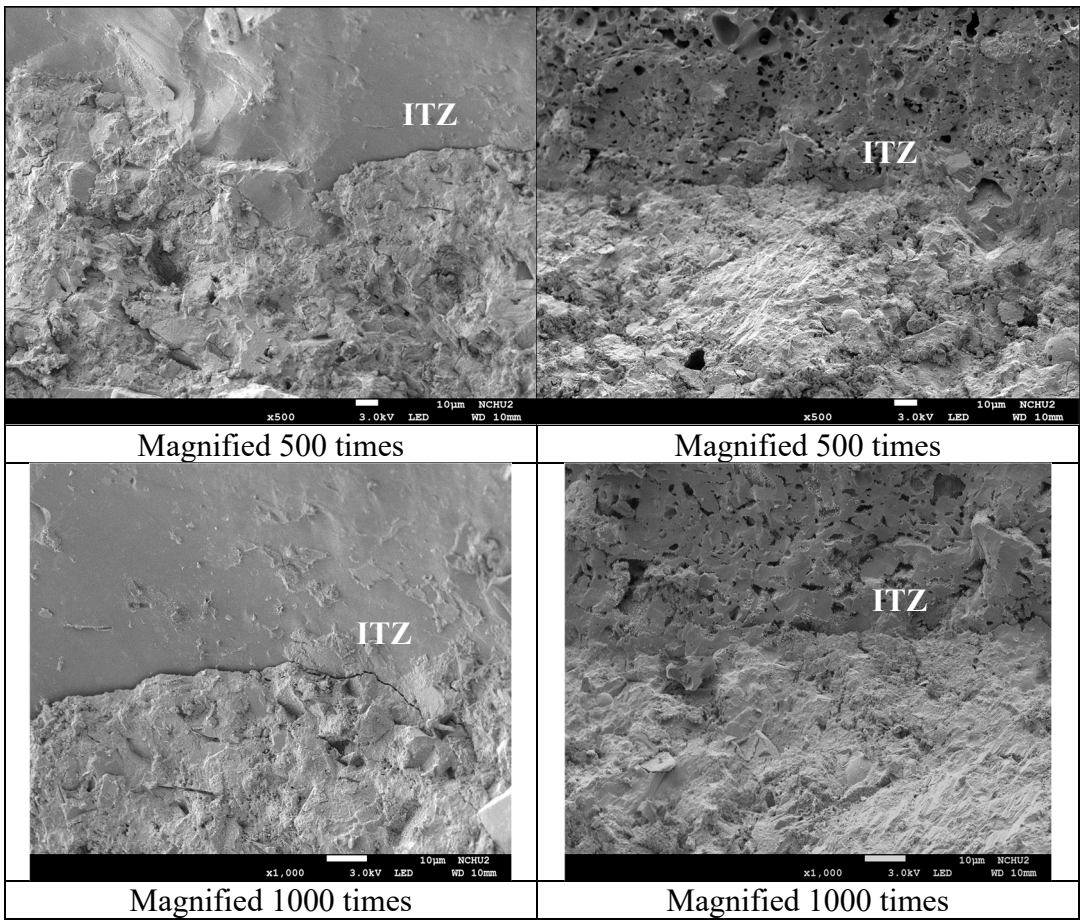

Figure 17. SEM micrographs of the concrete samples with a curing age of 90 days.

3.3. Results of Prestress Loss Monitoring of Prestressed Tendons

In this study, the prestress value, after the prestressed box girders were prestressed and anchored for 20 minutes, was used as the initial prestress. On the 3rd, 7th, 14th, 28th, 56th, 90th, 180th, 360th, 540th, and 720th days, a total of 11 times of prestress loss monitoring was carried out. The monitoring data are shown in Table 16. Among them, on the 720th day, the bridge was opened to traffic. When using the magnetic flux cable force measuring system to measure the prestress loss of the two groups of the prestressed box girders, it was found that the prestress loss occurred in the initial stage. However, at 180 days, it was found that the prestress increased slightly. This is because, after the preloading of the girder, there were other subsequent works on the bridge deck, such as the laying of the AC pavement and the erection of the guardrail in New Jersey. As a result, the static load of the bridge increased, leading to a rise in prestress.

Table 16. Prestress value in the magnetic flux monitoring prestressed box girder (unit: ton).

Installation Location		Monitoring Time (Day)										
		0	3	7	14	28	56	90	180	360	540	720
NC	Right side	376	364	362	369	361	361	357	377	350	353	346
LWC	Right side	265	252	253	254	254	260	271	271	252	260	254
	Left side	268	257	258	258	259	264	276	276	256	263	257

During the two years after prestressing, the prestress loss rate of the two groups of the prestressed box girders is shown in Table 17. It can be seen from Figure 18 that the prestress loss trends of the two groups of the prestressed box girders are similar. The largest prestress loss of the NC prestressed box girder occurred on the 720th day, and the prestress loss of magnetic flux reached 8.1%. In contrast, the largest prestress loss of the LWC prestressed box girder occurred on the 360th

Preprints (www.preprints.org) | NOT PEER-REVIEWED | Posted: 4 September 2023 doi:10.20944/preprints202309.0067.v1

day after prestressing, and the magnetic flux prestress loss monitoring values on both sides were 4.6% and 4.9%, respectively. Compared with the literature [19,38], the prestress loss of the two groups of prestressed box girders was not high. In particular, the prestress loss of the LWC prestressed box girder was smaller than that of the NC prestressed box girder.

Table 17. Percentage of the prestress loss in the magnetic flux monitoring prestressed box girder.

Installation Location		Monitoring Time (Day)										
		0	3	7	14	28	56	90	180	360	540	720
NC	Right side	0.0%	3.2%	3.8%	2.0%	4.0%	4.1%	5.1%	-0.3%	7.1%	6.1%	8.1%
LWC	Right side	0.0%	4.9%	4.6%	4.3%	4.1%	2.1%	-2.3%	-2.1%	4.9%	1.9%	4.2%
	Left side	0.0%	4.3%	3.8%	3.7%	3.5%	1.7%	-2.9%	-2.7%	4.6%	2.0%	4.1%

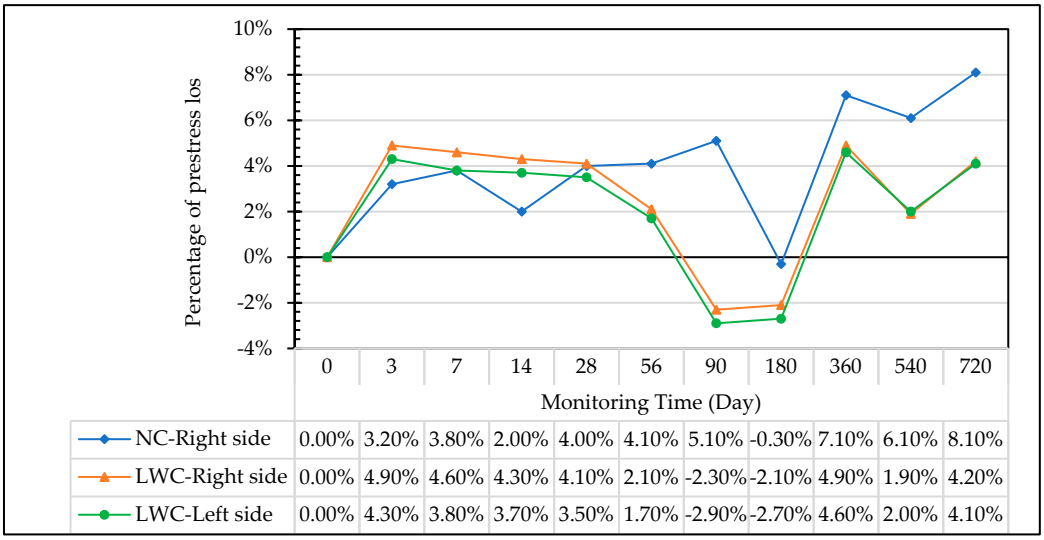

Figure 18. Relationship between the magnetic flux prestress loss percentages and monitoring times.

4. Conclusions

According to the above test and analysis results of the NC and LWC prestressed box girders, the following conclusions were drawn.

- The unit weight of the LWC was about 76%-78% of the NC, which could reduce the weight of the whole girder by more than 20%, thereby achieving the purpose of reducing the inertial force during earthquakes.
- Under standard curing conditions, the 28-day compressive strength of the LWC was 47.1 MPa, which met the requirements of ACI 213R-14. Under standard curing conditions, the 28-day flexural strength and 28-day splitting strength of the LWC were 3.5 and 3.0 MPa, which were 7.4% and 6.4% of its compressive strength, respectively.
- Under two different curing modes, the elastic modulus of the LWC at different curing ages ranged from 21.4 to 29.2 GPa (about 60-70% of that of NC), which is consistent with the literature.
- The LWAs in the LWC slowly released water into the matrix, which made the concrete more able to inhibit the early drying shrinkage, thus making the initial drying shrinkage smaller. However, the total dry shrinkage was comparable to the NC, and this was due to the lower elastic modulus of the LWC than that of NC, thus the initial creep was larger. In the later period, due to the small dry shrinkage, the total creep was equivalent to that of the NC.
- The ultrasonic pulse velocity of the LWC was lower than that of the NC of the same age. However, according to the recommendation of ASTM C597, the compactness of the LWC was rated as of a “good” quality.

- At the age of 28 days, the total charge of the LWC was 2889 coulombs, and the probability of chloride ion penetration was rated as "Moderate". However, at the age of 180 days, the total charge of the LWC was only 432 coulombs, and thus it was classified as having a "Very Low" chloride permeability.
- The increase in chloride ions in the LWC over a depth of 25 mm was much less than that in the NC. This indicated that the LWC could effectively resist chloride ion erosion.
- The SEM observation showed that the ITZ of the LWC had no visible interfacial cracks. These results confirmed that LWC can inhibit the infiltration of air, water, and chloride ions due to the strengthening of aggregates and cement paste in its ITZ, thus improving its durability.
- The magnetic flux prestress loss of the NC prestressed box girder reached 8.1%. In contrast, the monitored values of the magnetic flux prestress loss on both sides of the LWC prestressed box girder were 4.6% and 4.9%, respectively. This verified that, under the same environmental conditions, the use of LWC produced less of a prestress loss than the use of NC.

Author Contributions: Conceptualization, H.-J.C. and C.-C.K.; methodology, H.-J.C.; validation, H.-J.C., C.-C.K., and C.-W.T.; formal analysis, H.-J.C. and C.-C.K.; investigation, C.-C.K.; resources, H.-J.C.; data curation, H.-J.C.; writing—original draft preparation, H.-J.C. and C.-W.T.; writing—review and editing, C.-W.T.; visualization, H.-J.C.; supervision, H.-J.C.; project administration, H.-J.C.; funding acquisition, H.-J.C. All authors have read and agreed to the published version of the manuscript.

Funding: Not applicable.

Institutional Review Board Statement: Not applicable.

Informed Consent Statement: Not applicable.

Data Availability Statement: The data presented in this study are available on request from the corresponding authors.

Acknowledgments: The authors are grateful to the Freeway Bureau, Ministry of Transportation and Communications, Taiwan, for providing the experimental equipment and technical support.

Conflicts of Interest: The authors declare no conflicts of interest.

References

1. Mehta, P.K.; Monteiro, P.J.M. *Concrete: Microstructure, Properties, and Materials*, 3rd ed.; The McGraw-Hill Companies, Inc.: New York, NY, USA, 2006.
2. Mindess, S. and Young, J.F. *Concrete*; Prentice-Hall, Inc. Englewood Cliffs, New Jersey, pp. 521-532 (1981).
3. Chandra, S.; Berntsson, L. *Lightweight Aggregate Concrete*; NJ Noyes Publications: Norwich, UK, 2003.
4. DIN EN 13055. Leichte Gesteinskörnungen (Lightweight Aggregates); Beuth-Verlag: Berlin, Germany, 2016; p. 58.
5. Cheeseman, C.R.; Virdi, G.S. Properties and microstructure of lightweight aggregate produced from sintered sewage sludge ash. *Resour. Conserv. Recycl.* **2005**, *45*, 18–30.
6. Mun, K.J. Development and tests of lightweight aggregate using sewage sludge for nonstructural concrete. *Constr. Build. Mater.* **2007**, *21*, 1583–1588.
7. Chen, H.J.; Wang, S.Y.; Tang, C.W. Reuse of incineration fly ashes and reaction ashes for manufacturing lightweight aggregate. *Constr. Build. Mater.* **2010**, *24*, 46–55.
8. Tang, C.W.; Chen, H.J.; Wang, S.Y.; Spaulding, J. Production of synthetic lightweight aggregate using reservoir sediments for concrete and masonry. *Cem. Concr. Compos.* **2011**, *33*, 292–300.
9. Chen, H.J.; Yang, M.D.; Tang, C.W.; Wang, S.Y. Producing synthetic lightweight aggregates from reservoir sediments. *Constr. Build. Mater.* **2012**, *28*, 387–394.
10. Tang, C.W. Producing synthetic lightweight aggregates by treating waste TFT-LCD glass powder and reservoir sediments. *Comput. Concr.* **2014**, *13*, 325–342.
11. Chen, H.-J.; Hsueh, Y.-C.; Peng, C.-F.; Tang, C.-W. Paper Sludge Reuse in Lightweight Aggregates Manufacturing. *Materials* **2016**, *9*, 876. https://doi.org/10.3390/ma9110876
12. Chen, H.-J.; Chang, S.-N.; Tang, C.-W. Application of the Taguchi Method for Optimizing the Process Parameters of Producing Lightweight Aggregates by Incorporating Tile Grinding Sludge with Reservoir Sediments. *Materials* **2017**, *10*, 1294. https://doi.org/10.3390/ma10111294
13. Liu, M.; Wang, C.; Bai, Y.; Xu, G. Effects of sintering temperature on the characteristics of lightweight aggregate made from sewage sludge and river sediment. *Journal of Alloys and Compounds* **2018**, *748*, 522–

527. https://doi.org/10.1016/j.jallcom.2018.03.216
14. Porcino, D.D.; Mauriello, F.; Bonaccorsi, L.; Tomasello, G.; Paone, E.; Malara, A. Recovery of Biomass Fly Ash and HDPE in Innovative Synthetic Lightweight Aggregates for Sustainable Geotechnical Applications. *Sustainability* **2020**, *12*, 6552.
15. Lee, K.H.; Lee, K.G.; Lee, Y.S.; Wie, Y.M. Manufacturing and application of artificial lightweight aggregate from water treatment sludge. *J. Clean. Prod.* **2021**, *307*, 127260.
16. Nguyen, H.P.; Mueller, A.; Nguyen, V.T.; Nguyen, C.T. Development and characterization of lightweight aggregate recycled from construction and demolition waste mixed with other industrial by-products. *Constr. Build. Mater.* **2021**, *313*, 125472.
17. Tang, C.-W.; Cheng, C.-K. Sustainable Use of Sludge from Industrial Park Wastewater Treatment Plants in Manufacturing Lightweight Aggregates. *Materials* **2022**, *15*, 1785. https://doi.org/10.3390/ma15051785
18. Chen, H.-J.; Chang, W.-T.; Tang, C.-W.; Peng, C.-F. A Feasibility Study on Textile Sludge as a Raw Material for Sintering Lightweight Aggregates and Its Application in Concrete. *Appl. Sci* **2023**, *13*, 6395. https://doi.org/10.3390/app13116395
19. Chen, H.-J.; Wu, K.-C.; Tang, C.-W.; Huang, C.-H. Engineering Properties of Self-Consolidating Lightweight Aggregate Concrete and Its Application in Prestressed Concrete Members. *Sustainability* **2018**, *10*, 142. https://doi.org/10.3390/su10010142
20. ACI Committee 213. ACI 213R-14 Guide for Structural Lightweight-Aggregate Concrete; American Concrete Institute: Farmington Hills, MI, USA, 2014; p. 53.
21. Ramirez, J.A.; Olek, J.; Rolle, E.J.; Manlone, B.J. Performance of Bridge Decks and Girders with Lightweight Aggregate Concrete. Publication FHWA/IN/JTRP-98/17. Joint Transportation Research Program, Indiana Department of Transportation and Purdue University, West Lafayette, Indiana, 2000. https://doi.org/10.5703/1288284313288
22. Holm, T.A.; Bremmer, T.W.; De Souza, H. Aggregate-Matrix Interaction in Concrete Subjected to Severe Exposure. *Proceedings of the FIP/CPCI Symposia*, Canada, August 25-31, 1984.
23. Holm, T.A.; Bremmer, T.W.; Newman, J.B. Lightweight Concrete Subject to Severe Weathering. *Concrete International* **1984**, *6(6)*, pp. 49-54.
24. Holm, T.A.; Vaysburd, A.M. Structural Lightweight Aggregate Performance. *ACI SP-136*, **1992**, 424 pp.
25. Zhang, M.H.; Gjorv, O.E. Microstructure of the Interfacial Zone between Lightweight Aggregate and Cement Paste. *Cem Concr Res.* **1990**, *20*, 610-618.
26. Zhang, M.H.; Gjorv, O.E. Pozzolanic Reactivity of Lightweight Aggregates. *Cem Concr Res.* **1990**, *20*, 884-890.
27. Zhang, M.H.; Gjorv, O.E. Characteristics of Lightweight Aggregates for High-Strength Concrete. *ACI Materials Journal* **1991**, *88(2)*, 150-158.
28. Zhang, M.H.; Gjorv, O.E. Penetration of Cement Paste into Lightweight Aggregate. *Cem Concr Res.* **1992**, *22*, 47-55.
29. Swamy, R.N.; Lambert, G.H. The Microstructure of Lytag aggregate. *Int. j.* cem. compos. lightweight concr. **1981**, *3(4)*, 273-282.
30. Wasserman, R.; Bentur, A. Interfacial Interactions in Lightweight Aggregate Concrete and Their Influence on the Concrete Strength. *Cem Concr Compos* **1996**, *18*, 67-76.
31. Szydłowski, R.; Mieszczak, M. Study of application of lightweight aggregate concrete to construct posttensioned long-span slabs. *Procedia Eng.* **2017**, *172*, 1077–1085.
32. Thienel, K.-C.; Haller, T.; Beuntner, N. Lightweight Concrete—From Basics to Innovations. *Materials* **2020**, *13*, 1120. https://doi.org/10.3390/ma13051120
33. Zhang, M.-H.; Gjørv, O.E. Penetration of cement paste into lightweight aggregate. *Cem. Concr. Res.* **1992**, *22*, 47–55.
34. Lo, T.Y.; Cui, H.Z. Effect of porous lightweight aggregate on strength of concrete. *Materials Letters* **2004**, *58(6)*, 916–919.
35. Chen, H.-J.; Tsai, W.-P.; Tang, C.-W.; Liu, T.-H. Time-dependent properties of lightweight concrete using sedimentary lightweight aggregate and its application in prestressed concrete beams. *Struct. Eng. Mech.* **2011**, *39*, 833–847.
36. Chen, H.-J.; Liu, T.-H.; Tang, C.-W.; Tsai, W.-P. Influence of high-cycle fatigue on the tension stiffening behavior of flexural reinforced lightweight aggregate concrete beams. *Struct. Eng. Mech.* **2011**, *40*, 847–866.
37. Chen, H.J.; Yen, T.; Chen, K.H. Evaluating elastic modulus of lightweight aggregate. *ACI Materials Journal*

2003, *100(2)*, 108–113.
38. Szydłowski, R.S.; Łabuzek, B. Experimental Evaluation of Shrinkage, Creep and Prestress Losses in Lightweight Aggregate Concrete with Sintered Fly Ash. *Materials* **2021**, *14*, 3895. https://doi.org/10.3390/ma14143895
39. Bremner, T.W.; Holm, T.A. Elastic compatibility and the behavior of concrete. *ACI J.* **1986**, *83*, 244–250.
40. *LRFD Bridge Design Specifications*, 6th ed.; American Association of State Highway and Transportation Officials: Washington, DC, USA, 2012.
41. Neville, A.M. *Properties of Concrete*, 5th ed.; Pearson Education Limited: London, UK, 2012.
42. Ritthichauy, W.; Sugiyama, T.; Okamoto, T.; Tsuji, Y. Shear tests on reinforced lightweight aggregate concrete beams without web reinforcement. *Concrete Journal* **2001**, *23(3)*, 937–942.
43. ACI Committee 318, Building Code Requirements for Structural Concrete (ACI 318-14) and Commentary (ACI 318R–14), American Concrete Inst, Farmington Hills, MI, 2014.
44. Tian, Y.; Shi, S.; Jia, K.; Hu, S. Mechanical and dynamic properties of high strength concrete modified with lightweight aggregates presaturated polymer emulsion. *Constr. Build. Mater.* **2015**, *93*, 1151–1156.
45. Lotfy, A.; Hossain, K.M.; Lachemi, M. Durability properties of lightweight self-consolidating concrete developed with three types of aggregates. *Constr. Build. Mater.* **2016**, *106*, 43–54.
46. Wall, J.R. Non-traditional lightweight concrete for bridges, a lightweight aggregate manufacturers review of current practice. Proc. Conc. Bridge Conference, Portland Cement Association, Phoenix, AZ, 2010. P. 12.
47. Kraľovanec, J.; Bahleda, F.; Prokop, J.; Moravčík, M.; Neslušan, M. Verification of Actual Prestressing in Existing Pre-Tensioned Members. *Appl. Sci.* **2021**, *11*, 5971. https://doi.org/10.3390/app11135971
48. Moravˇcík, M. *Design of Prestressed Structures According to Eurocodes*, 1st ed.; EDIS: Žilina, Slovakia, 2017.
49. Hurst, M.K. Prestressed Concrete Design, 2nd ed.; E & FN SPON, An Imprint of Routledge: London, UK, 1998.
50. Bymaster, J.; Dang, C.; Floyd, R.; Hale, M. Prestress losses in pretensioned concrete beams cast with lightweight self-consolidating concrete. *Structures* **2015**, *2*, 50–57.
51. Wendling, A.; Sadhasivam, K.; Floyd, R.W. Creep and shrinkage of lightweight self-consolidating concrete for prestressed members. *Constr. Build. Mater.* **2018**, *167*, 205–215. https://doi.org/10.1016/j.conbuildmat.2018.02.017
52. Kayali, O.; Haque, M.N.; Zhu, B. Drying shrinkage of fibre-reinforced lightweight aggregate concrete containing fly ash. *Cem. Concr. Res.* **1999**, *29*, 1835–1840.
53. Kahn, L.F.; Lopez, M. Prestress losses in high-performance lightweight concrete pretensioned bridge girders. *PCI Struct. J.* **2005**, *50*, 84–94.
54. Shideler, J.J. Lightweight aggregate concrete for structural use. *Proceedings of Journal of the American Concrete Institute* **1957**, *54*, 298–328.
55. Short, A.; Kinniburgh, W. Lightweight Concrete. John Wiley & Sons, New York, USA, 1963.
56. Domagała, L.; Podolska, A. Effect of Lightweight Aggregate Impregnation on Selected Concrete Properties. *Materials* **2021**, *15*, 198.
57. Structural LWAC. Specification and Guideline for Materials and Production; Document BE96-3942/R14, Project Funded by the European Union under the Industrial & Materials Technologies Programme (Brite-EuRam III). 2000. Available online: https://www.researchgate.net/publication/339460461_LWAC_Material_Properties_-_State-of-the-Art
58. Nilsen, U.A.; Aitcin, P.C. Properties of high-strength concrete containing light-, normal-, and heavyweight aggregate. *Cem. Concr. Aggr.* **1992**, *14(1)*, 8–12.
59. Lopez, M.; Kahn L.F.; Kurtis, K.E. Creep and shrinkage of high performance lightweight concrete. *ACI Materials Journal* **2004**, *101(5)*, 391–399.
60. Rodacka, M.; Domagała, L.; Szydłowski, R. Assessment of Properties of Structural Lightweight Concrete with Sintered Fly Ash Aggregate in Terms of Its Suitability for Use in Prestressed Members. *Materials* **2023**, *16*, 5429. https://doi.org/10.3390/ma16155429
61. EN 1992 Eurocode 2; Design of Concrete Structures—Part 1-1: General Rules and Rules for Buildings. European Committee for Standardization: Brussels, Belgium, 2013.
62. Lopez, M.; Kahn, L.; Kurtis, K.; Lai, J. Creep, Shrinkage, and Prestress Losses of High-Performance Lightweight Concrete; GDOT Research Project No. 2004; Office of Materials and Research Georgia Department of Transportation: Atlanta, GA, USA, 2003.
63. Lopez, M.; Kurtis, K.; Kahn, L. Pre-wetted lightweight coarse aggregate reduces long-term deformations of

high performance lightweight concrete. In Proceedings of the 7th CANMET/ACI International Conference on Durability of Concrete, SP-234, Montreal, QC, Canada, 28 May–3 June 2006.

64. Kayali, O. Fly ash lightweight aggregates in high performance concrete. *Constr. Build. Mater.* **2008**, *22(12)*, 2393–2399. https://doi.org/10.1016/j.conbuildmat.2007.09.001
65. *Standard Test Method for Relative Density (Specific Gravity) and Absorption of Coarse Aggregate*; ASTM C127/C127M-15; ASTM International: West Conshohocken, PA, USA, 2015. Available online: https://www.astm.org/Standards/C127 (accessed on 13 March 2023)
66. *Method of test for the particle cylindrical crushing strength of lightweight coarse aggregates*; CNS 14779; Bureau of Standards, Metrology and Inspection, Ministry of Economic Affairs, R.O.C., Taiwan, 2021.
67. *Method of test for resistance to degradation of coarse aggregate (smaller then 37.5 mm) by abrasion and impact in the Los Angeles machine*; CNS 490; Bureau of Standards, Metrology and Inspection, Ministry of Economic Affairs, R.O.C., Taiwan, 2021.
68. *Method of Test for Soundness of Aggregate by Use of Sodium Sulfate or magnesium Sulfate*; CNS 1167; Bureau of Standards, Metrology and Inspection, Ministry of Economic Affairs, R.O.C., Taiwan, 2018.
69. *Lightweight aggregates for structural concrete*; CNS 3691; Bureau of Standards, Metrology and Inspection, Ministry of Economic Affairs, R.O.C., Taiwan, 2019.
70. *Standard Test Method for Determining Density of Structural Lightweight Concrete;* ASTM C567/C567M-19; ASTM International: West Conshohocken, PA, USA, 2019. Available online: https://www.astm.org/Standards/C567 (accessed on 12 March 2023)
71. *Standard Test Method for Compressive Strength of Cylindrical Concrete Specimens*; ASTM C39/C39M-18; ASTM International: West Conshohocken, PA, USA, 2018. Available online: https://www.astm.org/Standards/C39 (accessed on 12 March 2023)
72. *Standard Test Method for Flexural Strength of Concrete (Using Simple Beam with Third-Point Loading)*; ASTM C78/C78M-09; ASTM International: West Conshohocken, PA, USA, 2009. Available online: https://www.astm.org/Standards/C78 (accessed on 12 March 2023)
73. *Standard Test Method for Splitting Tensile Strength of Cylindrical Concrete Specimens*; ASTM C496/C496M-96; ASTM International: West Conshohocken, PA, USA, 1996. Available online: https://www.astm.org/Standards/C496 (accessed on 12 March 2023)
74. *Standard Test Method for Static Modulus of Elasticity and Poisson's Ratio of Concrete in Compression*; ASTM C469/C469M-14; ASTM International: West Conshohocken, PA, USA, 2014. Available online: https://www.astm.org/Standards/C469 (accessed on 13 March 2023)
75. *Standard Test Method for Length Change of Hardened Cement Mortar and Concrete*; ASTM C157/C157M-08; ASTM International: West Conshohocken, PA, USA, 2008. Available online: https://www.astm.org/Standards/C157 (accessed on 13 March 2023)
76. *Standard Test Method for Creep of Concrete in Compression*; ASTM C512/C512M-15; ASTM International: West Conshohocken, PA, USA, 2015. Available online: https://www.astm.org/Standards/C512 (accessed on 13 March 2023)
77. *Standard Test Method for Pulse Velocity Through Concrete*; ASTM C597-16; ASTM International: West Conshohocken, PA, USA, 2016. Available online: https://www.astm.org/Standards/C597 (accessed on 14 March 2023)
78. *Method of test for electrical indication of concrete's ability to resist chloride ion penetration*; CNS 14795; Bureau of Standards, Metrology and Inspection, Ministry of Economic Affairs, R.O.C., Taiwan, 2020.
79. *Standard Test Method for Determining the Penetration of Chloride Ion into Concrete by Ponding*; ASTM C1543-10; ASTM International: West Conshohocken, PA, USA, 2010. Available online: https://www.astm.org/Standards/C1543 (accessed on 14 March 2023).
80. *Method of test for resistance of concrete to chloride ion penetration*; CNS 15649; Bureau of Standards, Metrology and Inspection, Ministry of Economic Affairs, R.O.C., Taiwan, 2019.
81. *Method of test for acid-soluble chloride in mortar and concrete*; CNS 14702; Bureau of Standards, Metrology and Inspection, Ministry of Economic Affairs, R.O.C., Taiwan, 2021.
82. Wang, Y.; Xiao, R.; Lu, H.; Hu, W.; Jiang, X.; Huang, B. Effect of curing conditions on the strength and durability of air entrained concrete with and without fly ash. *Cleaner Materials* **2023**, *7*, 100170, https://doi.org/10.1016/j.clema.2023.100170
83. Al-Khaiat, H.; Haque, M.N. Effect of initial curing on early strength and physical properties of a lightweight concrete. *Cem. Concr. Res.* **1998**, 28(6), 859–866.

84. Nilsen, A.U.; Monteiro, P.J.M.; Gjørv, O.E. Estimation of the elastic moduli of lightweight aggregate. *Cem. Concr. Res.* **1995**, *25(2)*, 276–280. https://doi.org/10.1016/0008-8846(95)00009-7
85. Holste, J.R.; Peterman, R.J.; Esmaeily, A. Evaluating the Time-Dependent and Bond Characteristics of Lightweight Concrete Mixes for Kansas Prestressed Concrete Bridges, Research Report KSU-08-02, Kansas State University Transportation Center, 2011.
86. Chen, H.-J.; Chen, Y.-C.; Tang, C.-W.; Lin, X.-F. The Corrosion Resistance of Reinforced Lightweight Aggregate Concrete in Strong Brine Environments. *Materials* **2022**, *15*, 7943. https://doi.org/10.3390/ma15227943